

**DAMAGE PRODUCTION BY FAST ELECTRONS IN DILUTE ALLOYS
OF VANADIUM, NIOBIUM AND MOLYBDENUM**

P. JUNG and G. LUCKI

PUBLICAÇÃO IEA N.º 391
Abril — 1975

INSTITUTO DE ENERGIA ATÔMICA
Caixa Postal 11049 (Pinheiros)
CIDADE UNIVERSITÁRIA "ARMANDO DE SALLES OLIVEIRA"
SÃO PAULO — BRASIL

**DAMAGE PRODUCTION BY FAST ELECTRONS IN DILUTE ALLOYS
OF VANADIUM, NIOBIUM AND MOLYBDENUM**

P. Jung* and G. Lucki

**Coordenadoria de Ciência e Tecnologia de Materiais
Instituto de Energia Atômica
São Paulo - Brasil**

**Publicação IEA Nº 391
Abril - 1975**

* Institut für Festkörperforschung der Kernforschungsanlage Jülich, Germany.

Instituto de Energia Atômica

Conselho Superior

Eng^o Roberto N. Jafet - Presidente
Prof. Dr. Emilio Mattar - Vice-Presidente
Prof. Dr. Jose Augusto Martins
Prof. Dr. Milton Campos
Eng^o Helcio Modesto da Costa

Superintendente

Prof. Dr. Rômulo Ribeiro Pieroni

DAMAGE PRODUCTION BY FAST ELECTRONS IN DILUTE ALLOYS OF VANADIUM, NIOBIUM AND MOLYBDENUM

P. Jung and G. Lucki

ABSTRACT

Vanadium, niobium and molybdenum samples containing about 300 ppm of zirconium were irradiated at helium temperature with electrons of energies between 0.6 and 3.1 MeV. The measured damage rates were analysed in terms of minimum threshold energy, damage function and resistivity per unit concentration of Frenkel pairs. For the minimum threshold energy T_d , values of 25 ± 2 eV (V), 28 ± 2 eV (Nb) and 34 ± 2 eV (Mo) were obtained.

Pronounced differences between the displacement functions of molybdenum and that of niobium and vanadium are found which are explained by different stability of the defects during the irradiation at helium temperature.

Introduction

This work is part of an interlaboratory program to study low temperature damage rates in dilute vanadium, niobium and molybdenum alloys after irradiation with electrons, protons, fission neutrons and 14 MeV neutrons. The samples were prepared by R. E. Reed of Oak Ridge National Laboratory and a detailed description of sample preparation is given elsewhere⁽¹⁶⁾.

The main reason why dilute alloys instead of high purity materials were chosen, was to suppress transient variation in the apparent damage rate that is observed at low dose in high purity bcc-materials. Another problem that occurs in high purity bcc material is that they show strong texture after annealing treatment for purification. This fact is the main reason for irreproducible damage rates in high purity specimen^(13,17) and can be explained by the strong anisotropy of defect production rates in bcc metals^(6,1). For these reasons the samples were prepared with a content of about 300 ppm of zirconium and were used in a not fully recrystallized condition. The room to helium temperature resistivity ratios were about 110 (V), 70 (Nb) and 75 (Mo), respectively. The thicknesses were about 35 μm (V), 33 μm (Nb) and 28 μm (Mo), respectively, with variations of about 2 μm .

Irradiation and resistivity measurement were done at 4.5 K. Transverse magnetic fields of 1.8 kOe for vanadium and 10 kOe for niobium were applied to suppress superconductivity in these specimens. The flux of irradiation electrons was determined by simultaneously irradiating aluminum wires of 200 μm diameter. Damage rate data of aluminum are well known from measurements of different authors^(15,18) and were checked in an earlier work⁽⁶⁾ in our laboratory. For the energies used in this work, the corresponding aluminum data are given in Table I. The electron energy in the middle of the specimen, which is given in Table I is about 0.05 MeV lower than the accelerator energy. This is caused by energy degradation in a 12 μm stainless steel window, about 1 mm liquid helium in front of the specimen, and by energy loss in the front part of the specimen. Corrections for the influence of beam spreading are not necessary, as beam spreading in the aluminum and in the other specimen is nearly the same and therefore is canceled when the damage rates are calculated.

Results

Fig. 1 shows damage rates, that is resistivity increase per incident flux of irradiation electrons as a function of irradiation induced resistivity for the three sample materials and for different energies as indicated. Some of the curves show in the region of very low doses a bending off to higher values. This initial behaviour was not reproducible. Therefore the damage rates above about $2 \text{ n}\Omega\text{cm}$ corresponding to electron fluxes of $5 \cdot 10^{16} \text{ electrons/cm}^2$, were extrapolated to zero damage

The initial damage rates obtained by extrapolation are shown in the figures 2 to 4 as a function of energy. The abscissa T_{max} is the maximum energy, an irradiation electron can transfer to a lattice atom.

In the figures also results are inserted, which have been obtained for pure materials by other authors. In the case of vanadium, recent results of Miller and Chaplin⁽¹⁴⁾ do well continue our results to the low energy region. For niobium Faber's⁽⁴⁾ results are close to our results, while the results of Youngblood et al⁽¹⁹⁾ cannot be compared directly, as these authors irradiated at about 25 k.

In the case of molybdenum our low-energy results can be compared with the data obtained by Lucasson and co-workers^(11,17). From their new results⁽¹¹⁾, we find good agreement with their less pure (VP)-material, while their high-purity (Marz-grade) molybdenum showed a pronounced texture and therefore cannot be regarded as truly polycrystalline.

In conclusion, we see that our samples show damage rate versus energy curves which are identical to those of pure polycrystalline material within experimental error.

Discussion

For the interpretation of damage rate data the so-called damage function $P(T)$ is used which is defined by

$$\frac{\Delta\rho}{\Delta\phi}(T_{\text{max}}(E)) = \rho_F \cdot \int_{T_d}^{T_{\text{max}}(E)} P(T) \cdot \frac{d\sigma}{dT}(E,T) dt \quad (1)$$

$\frac{\Delta\rho}{\Delta\phi}$ is the measured damage rate, $\frac{d\sigma}{dT}$ is the differential scattering cross section for electrons given by Mott, T_d is the threshold energy for damage production and ρ_F is a parameter which describes the resistivity per unit concentration of Frenkel pairs. That means, $P(T)$ gives the average number of stable Frenkel pairs, which are produced by an energy transfer T from an irradiation electron of energy E to a lattice atom.

From equation (1) it is directly seen, that $P(T)$ can be determined only within the constant factor ρ_F .

Some assumptions about $P(T)$ can be made: By definition $P(T)$ is equal to zero for $T < T_d$ and is expected to increase monotonically with T . Furtheron from computer calculations of the Brookhaven group^(3, 5) it may be assumed that $P(T)$ passes the unity value for T -values around three to five times the threshold energy. Finally from theoretical considerations on multiple

displacement (compare Ref ⁽⁹⁾) a linear increase of $P(T)$ may be expected for energies far above threshold.

In this work the data were evaluated by replacing $P(T)$ in equation(1) by a multiple step function, with steps at the irradiation energies used in this experiment. The corresponding $P(T)$ values are then directly obtained by replacing the integral by a sum. This method was already applied by Wurm⁽¹⁸⁾ and is only well applicable at low energies while at higher energies small experimental errors may cause large changes in $P(T)$. The dependence of $P(T)$ on the damage rate curve is shown in Fig. 5, where the measured damage rates of niobium are approximated by an increasing number of steps of the $\rho_F P(T)$ function. While the first steps cause appreciable changes in the calculated damage rate curve, the last additional step changes the calculated curve only within the experimental error. That means, at higher energies, $\rho_F P(T)$ cannot be derived from experimental data with sufficient accuracy by this technique, if no further assumptions are made.

Finally, to obtain only $P(T)$, it is necessary to make assumptions about ρ_F . As very little is known about the resistivity contribution of an interstitial, only a lower limit of ρ_F may be estimated from the resistivity of a vacancy ρ_V , which in principle can be obtained from quenching experiments. On the other hand for most fcc metals reasonable $P(T)$ values were obtained by setting ρ_F equal to the 0°C-resistivity value, according to a proposal made by Lucasson and Walker⁽¹²⁾. Therefore we divided our $\rho_F P(T)$ curves by the resistivities at room temperature, which are quoted in Table II. The results of this procedure are shown in Fig. 6, where also the results for two other bcc metals Fe and Ta are given. For iron the damage rate data of Lucasson and Walker⁽¹¹⁾ and for tantalum the data of Meissner⁽¹³⁾ were used. For comparison also curves for two fcc-metals are inserted. The $P(T)$ function of copper was obtained by Wurm et al⁽¹⁸⁾ and that of platinum is derived from measurements in our institute⁽⁷⁾. Finally, the dashed lines correspond to $P(T)$ functions derived from computer simulations for α -iron of the Brookhaven group⁽³⁾, and from our single crystal measurements on tantalum⁽⁶⁾, respectively. In these last two curves no assumptions about ρ_F were involved.

The abscissa in Fig. 6 is normalized by the respective threshold energies T_d , which are given also in Table II. We see that the $P(T)$ functions of the VB-metals V, Nb and Ta and also the theoretical curve for α -iron (Fe^*) as well as the single crystal curve for tantalum (Ta^*) show qualitatively similar behaviour, and are raising somewhat slower than the curves for the fcc-metals. On the other hand the curves of Fe and Mo are increasing much steeper, reaching unity already at energies of about $2 T_d$, while the $P(T)$ functions of the VB-metals need energies around 4 to 5 times T_d to reach this value.

At moment only speculations are possible about the reason of this difference.

The one possibility, which was proposed in Ref (17), is that the $\rho_F/\rho_{22^\circ C}$ -values of iron and especially molybdenum are by a factor of about 2 higher than for the VB metals and the fcc-metals. On the other hand, we expect that differences in the $\rho_F/\rho_{22^\circ C}$ -relation should not cause the large differences in Fig. 6 between the VB metals and the other bcc metals, iron and molybdenum. We expect from the large differences in the annealing behaviour of iron and molybdenum on one side and the VB metals on the other side, that the stability of defects at helium temperature is quite different for both groups of metals. That means, the $P(T)$ -function themselves may be rather different, irrespective of small differences in the $\rho_F/\rho_{22^\circ C}$ -values.

Finally from the data of Fig 1 saturation values for defect production can be derived. By extrapolating the curves to zero damage rate one obtains the saturation resistivity ρ_s , and furtheron the saturation concentration of defects by

$$c_s = \rho_s / \rho_F \quad (2)$$

This extrapolation is only possible for the 2.8 MeV irradiation where enough damage was accumulated during the irradiation time. In the case of vanadium, both 2.8 MeV irradiations which were done on different specimen showed a much faster decrease than the curves of the 1.2 and 1.9 MeV irradiation, which show a decrease similar to that of the curves of niobium and molybdenum. To decide whether this behaviour of the 2.8 MeV vanadium curves is continued to higher defect concentrations or whether the curves are bending off, time consuming irradiations would be necessary.

With the reservations quoted above we use $\rho_{22^\circ\text{C}}$ instead of ρ_F and obtain the c_s values in the last column of Table II. Generally the c_s values may be in error by at least a factor of 2. Within these limits they agree well with the data for the fcc materials aluminum, copper and platinum where values around 0.4 at% have been reported⁽²⁾.

Table I

Measured damage rates $\frac{\Delta\rho}{\Delta\phi}$ of vanadium, niobium and molybdenum, containing 300 ppm of zirconium. The aluminum data are interpolated from results in Refs. ⁽¹⁵⁾ and ⁽¹⁹⁾ and were used to determine the electron flux. E corresponds to the energy of the electrons in the middle of the samples, the damage rate values are given in units of $10^{-26} \Omega\text{cm}^3$.

E [MeV]	V (Zr)	Nb (Zr)	Mo (Zr)	Al
0.55	0.30	0.00	0.00	0.42
0.65	0.55	0.00	0.00	0.46
0.75	0.74	0.05	0.00	0.50
0.85	0.92	0.21	0.007	0.53
0.95	1.15	0.46	0.07	0.57
1.15	1.59	0.86	0.42	0.65
1.35	2.03	1.22	0.90	0.72
1.55	2.40	1.64	1.40	0.79
1.85	3.00	2.26	2.11	0.88
2.15	3.58	2.90	2.96	0.94
2.45	4.03	3.51	3.80	1.00
2.75	4.38	4.09	4.52	1.05
3.05	4.71	4.67	4.87	1.09

Table II

Threshold energies for defect production T_d , room temperature resistivity values $\rho_{22^\circ\text{C}}$ and saturation values for defect production c_s .

	T_d [eV]	$\rho_{22^\circ\text{C}}^{a)}$ [$10^{-6} \Omega\text{cm}$]	c_s [at%]
V (Zr)	25 ± 2	19.9	?
Nb (Zr) ^{b)}	28 ± 2	14.5	0.23
Ta ^{c)}	32 ± 2	13.1	0.27
Fe ^{d)}	20 ± 2	9.8	-
Mo (Zr)	34 ± 2	5.3	0.37

Figure Captions

Fig. 1 Damage rate versus resistivity increase observed for V, Nb and MO during electron irradiation at 4.5 k and energies of 1.2, 1.9 and 2.8 MeV (and x).

Fig. 2 Initial damage rates of vanadium (+ 300 ppm Zr) as a function of the maximum transferred energy. The solid line corresponds to calculated values, using the $\rho_F \cdot P(T)$ -function show in Fig. 6. The (x)-values correspond to results for pure vanadium given in Ref.(14).

Fig. 3 Initial damage rates of niobium (+ 300 ppm Zr) as a function of the maximum transferred energy. The solid line corresponds to calculated values, using the $\rho_F \cdot P(T)$ -function shown in Fig. 6. The (x)- and (+)-values correspond to results for pure niobium given in Refs.(14) and (19), respectively.

Fig. 4 Initial damage rates of molybdenum (+ 300 ppm Zr) as a function of the maximum transferred energy. The solid line corresponds to calculated values, using the $\rho_F \cdot P(T)$ -function show in Fig. 6. The (+)- and (x)-values correspond to results for pure molybdenum given in Refs.(11) and (17), respectively. The values of Ref.(11) are corrected for simultaneous annealing during the irradiation at 20 k.

Fig. 5 Stepwise approximation of the averaged damage rate curve of niobium (lower part) by a $\rho_F \cdot P(T)$ step function (upper part).

Fig. 6 $P(T)$ -functions for V, Nb and Mo obtained by deviding $\rho_F \cdot P(T)$ by the room-temperature resistivity $\rho_{22^\circ\text{C}}$. On the abszissa T_{max} is divided by the respective threshold energies T_d . The curves for iron (Fe) and tantalum (Ta) are derived from data given in Refs.(11) and (13) respectively. The Fe^{*}-curve corresponds to results of computer calculation for α -iron in Ref.(3) the Ta^{*}-curve is the $P(T)$ -function derived from single crystal experiments on tantalum in Ref.(8). The curves for fcc-metals are from Ref.(18) (Cu) and from measurements in our institute (7) (Pt), respectively.

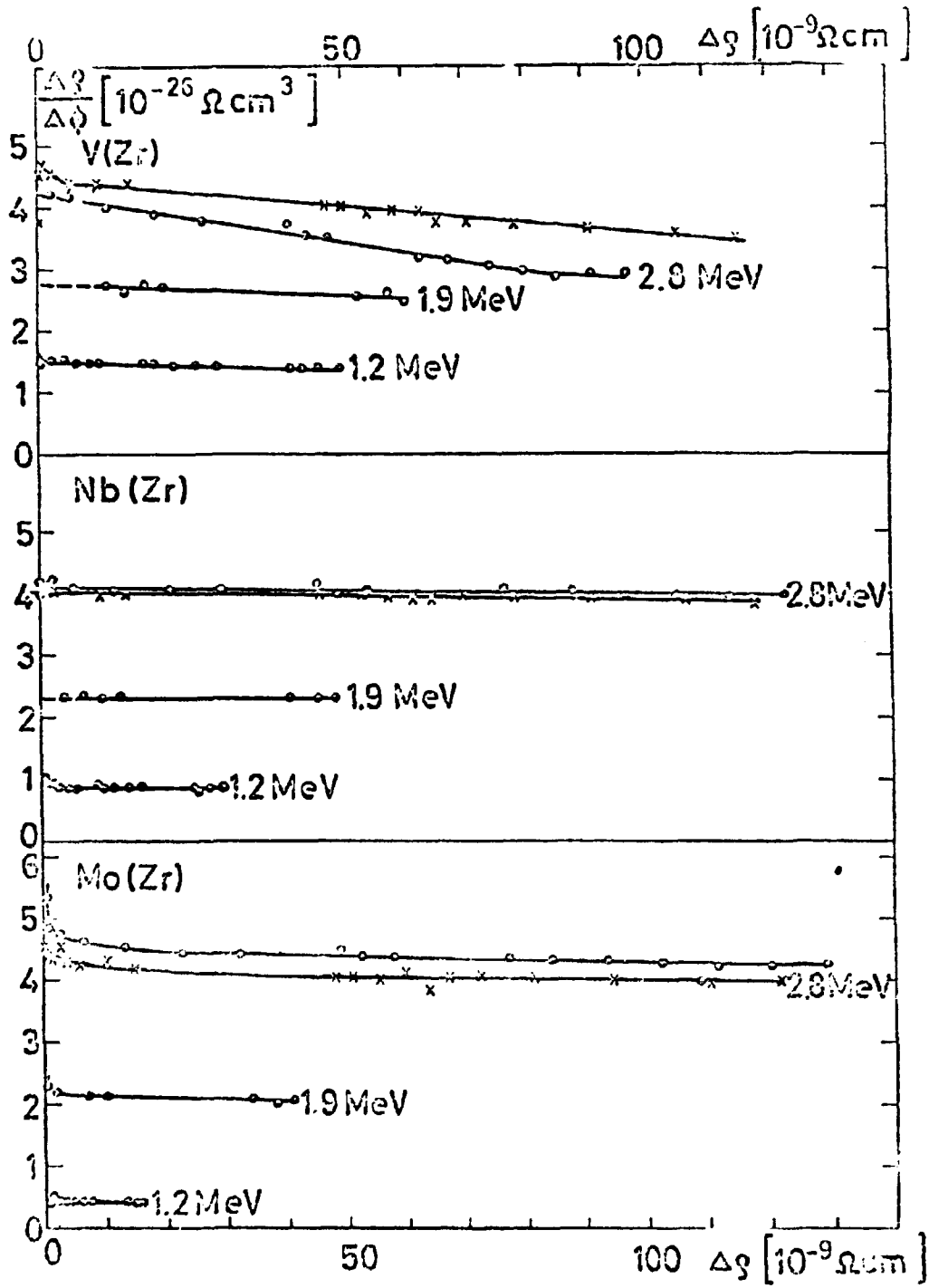


Figure 1

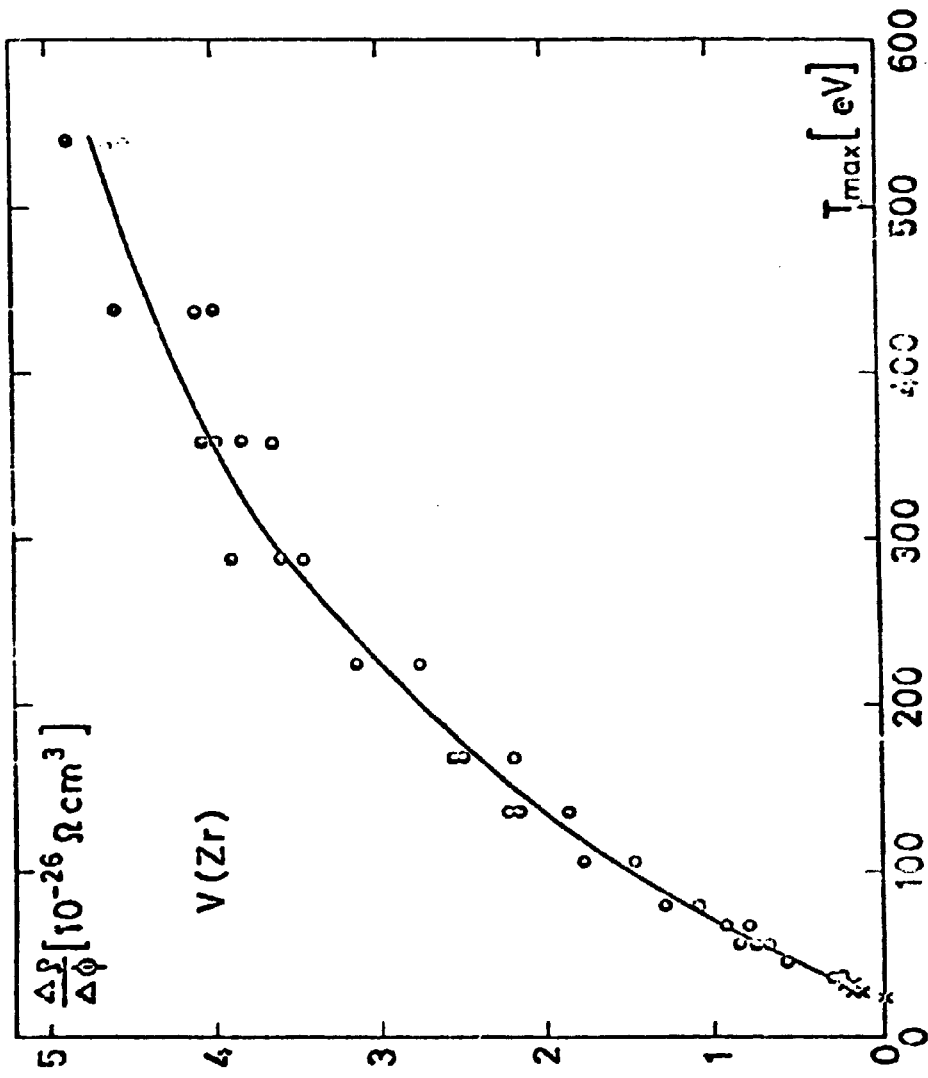


Figure 2

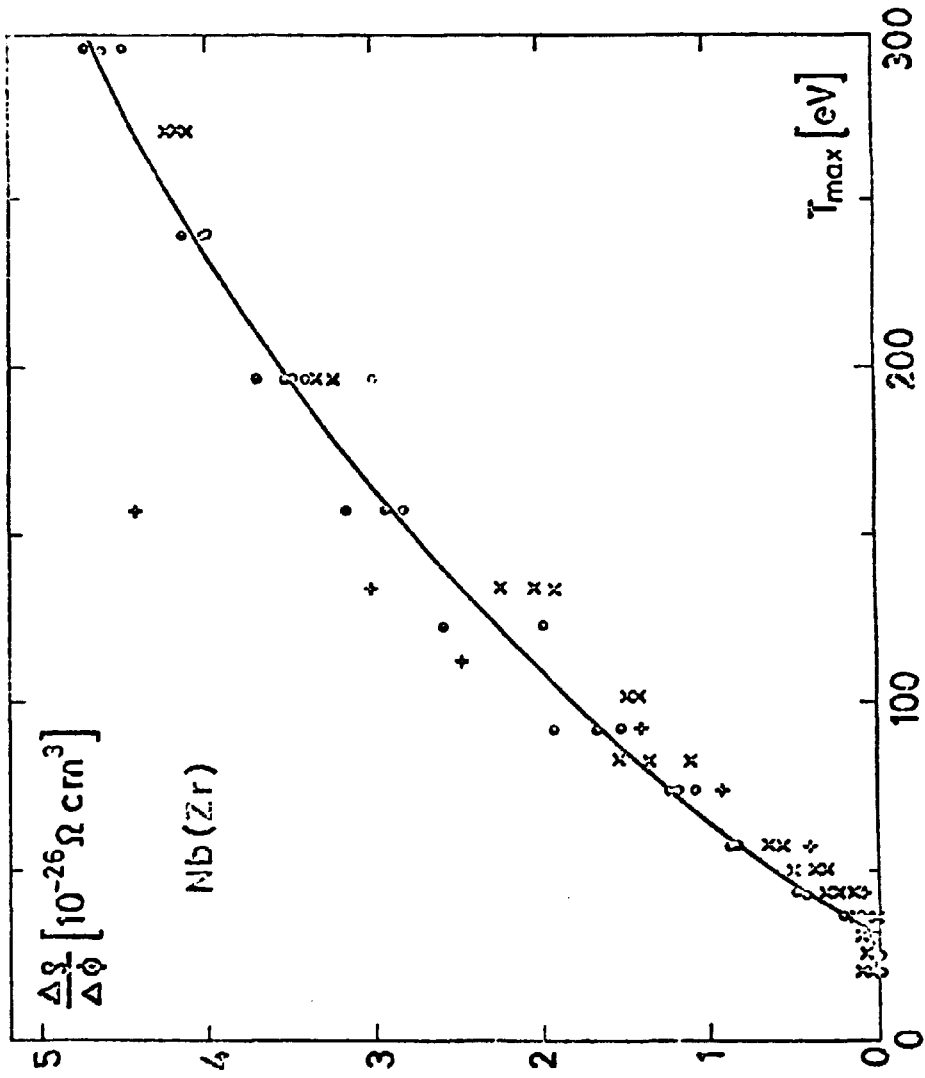


Figure 3

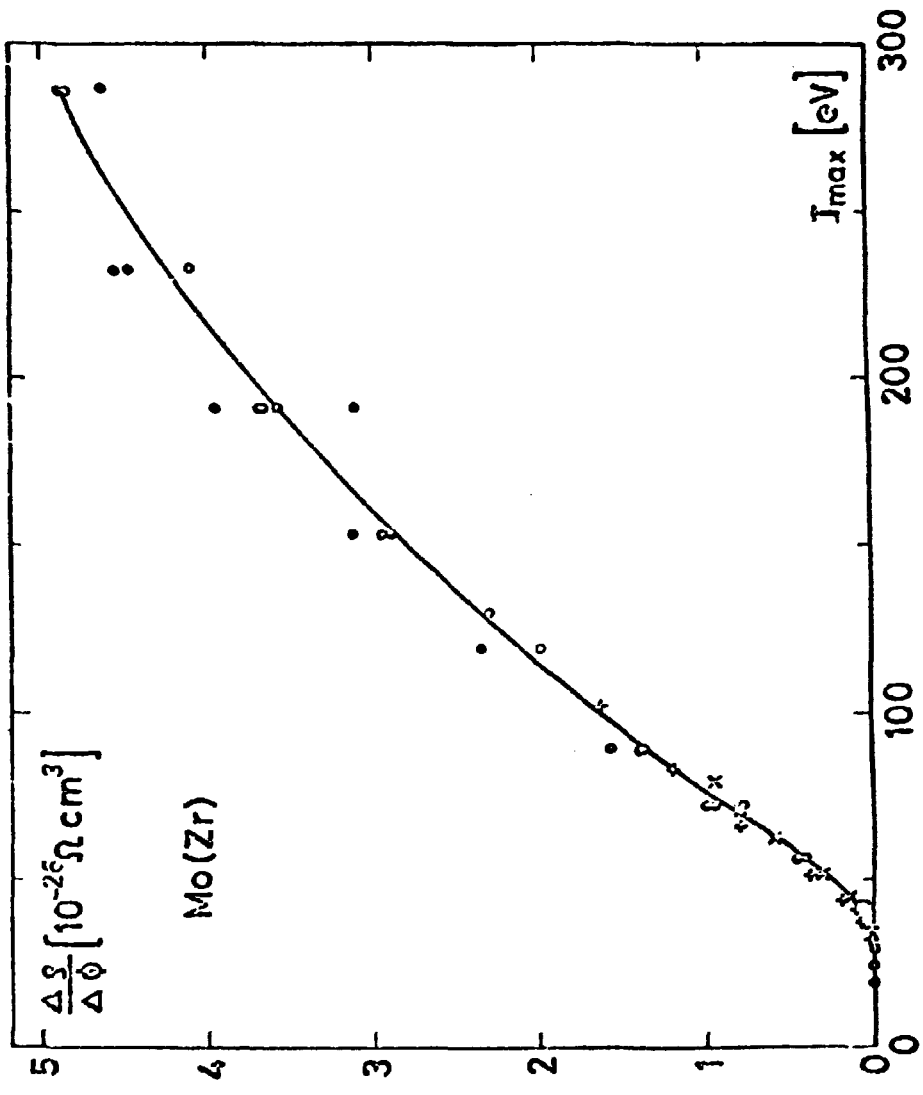


Figure 4

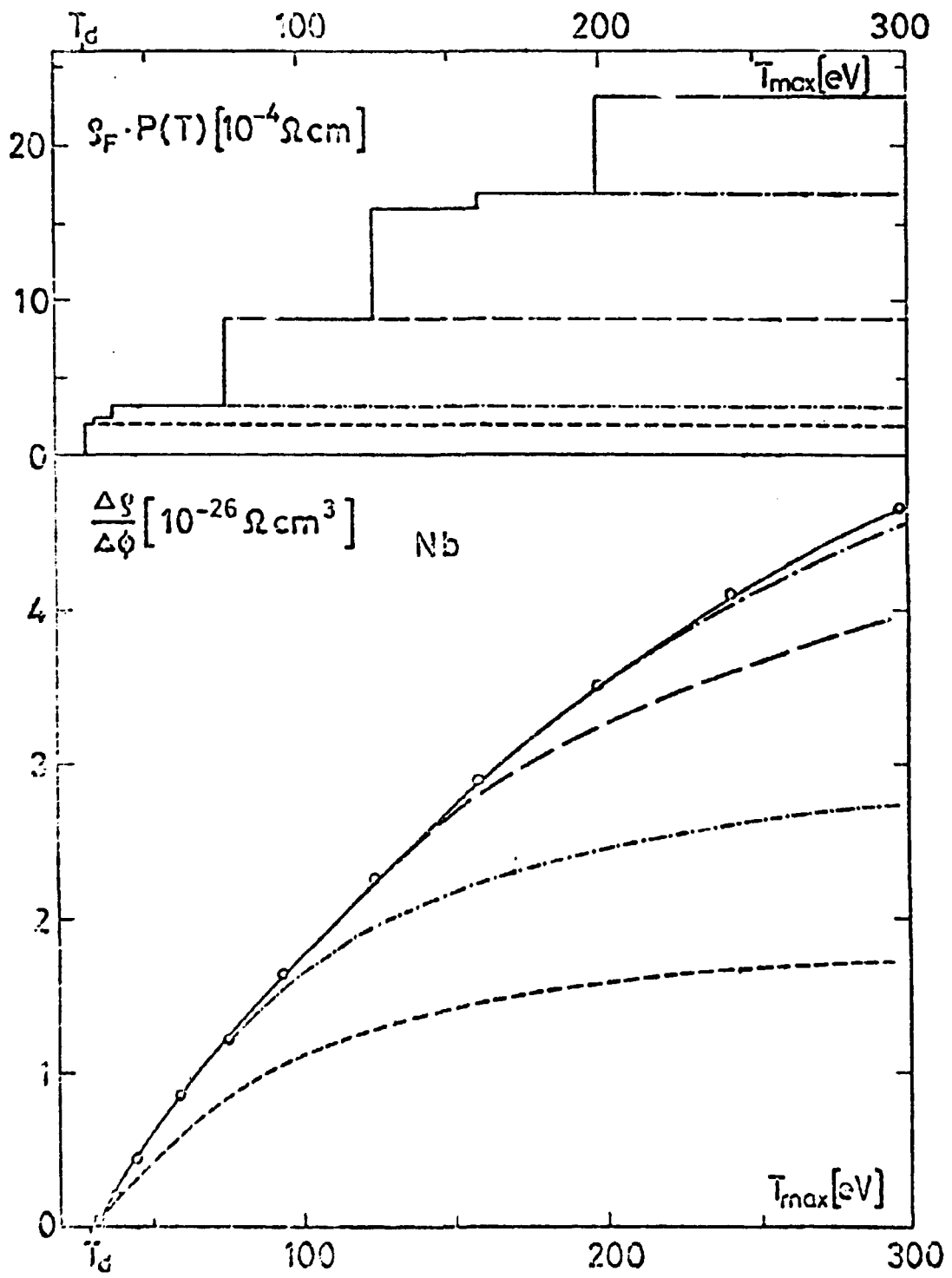


Figure 5

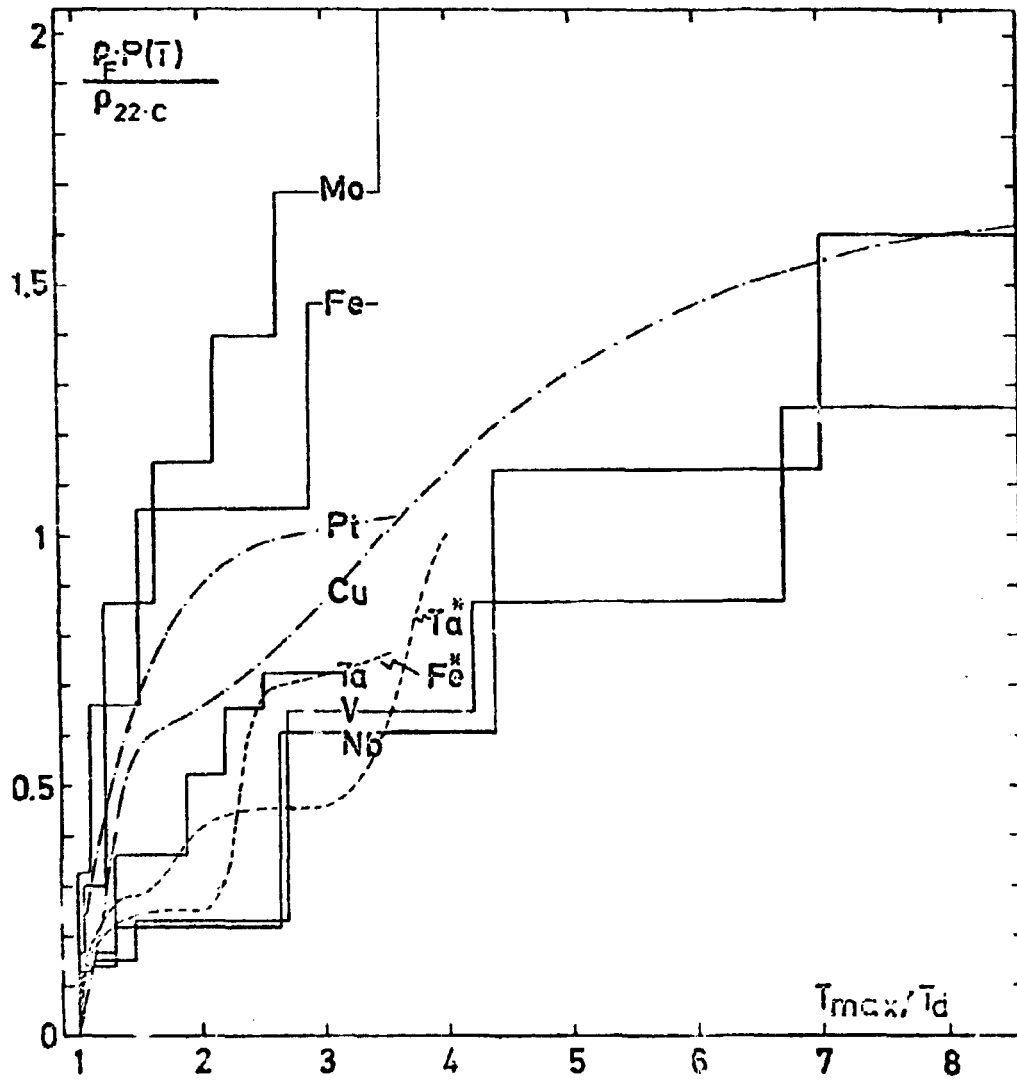


Figure 6

RESUMO

Amostras de vanádio, nióbio e molibdênio contendo aproximadamente 300 ppm de zircônio foram irradiadas com elétrons com energias compreendidas entre 0,6 e 3,1 MeV, à temperatura de hélio líquido. As taxas de irradiação medidas foram analisadas em termos da energia de limiar mínima, função de dano e da resistividade para concentração unitária de pares de Frenkel. Para a energia de limiar mínima foram obtidos os seguintes valores: 25 ± 2 eV (V), 28 ± 2 eV (Nb), e 34 ± 2 eV (Mo).

As pronunciadas diferenças encontradas entre as funções de dano para o molibdênio e as do nióbio e vanádio são explicadas pela diferente estabilidade dos defeitos durante a irradiação a temperatura do hélio líquido.

RESUMÉ

Des échantillons de niobium, vanadium et molybdène contenant environ 300 ppm de zirconium ont été irradiés à la température de l'hélium liquide par des électrons d'énergies comprises entre 0,6 et 3,1 MeV. Les taux de dommage mesurés ont été analysés en termes de l'énergie de seuil minimum, de la fonction de dommage et de la resistivité des paires de Frenkel par unité de volume. Pour l'énergie de seuil minimum T_D , on obtient les valeurs suivantes: 25 ± 2 eV (V), 28 ± 2 eV (Nb) et 34 ± 2 eV (Mo).

Les grandes différences observées entre les fonctions de déplacement du Mo et celles du Nb et du V sont expliquées par des différences de stabilité des défauts pendant l'irradiation à la température de l'hélium liquide.

REFERENCES

1. BIGET, B. et alii. A study of electron irradiation damage in single crystals of molybdenum. *Radiat. Effects*, London, **21**:229-34, 1974.
2. DUESING, et alii. Defect production during low temperature electron irradiation. 2. The influence of radiation doping on the defect production in aluminium, copper, and platinum. *Crys. Lattice Defects*, London, **1**:135-44, 1969.
3. ERGINSOY, G. H. et alii. Dynamics of radiation damage in a body-centered cubic lattice. *Phys. Rev. A*, Ithaca, N. Y., **133**(2):A595-A606, 1964.
4. FABER, K. [Title unknown]. Stuttgart, Universität, 1974 [Thesis].
5. GIBSON, J. B. et alii. Dynamics of radiation damage. *Phys. Rev.*, Ithaca, N. Y., **120**(4):1229-53, 1960.
6. JUNG, P. & SCHILLING, W. Anisotropy of the threshold energy for the production of Frankel pairs in tantalum. *Phys. Rev. B*, Ithaca, N. Y., **5**(6):2046-56, 1972.
7. JUNG, P. et alii. Anisotropy of the threshold for production of Frankel pairs in copper and platinum. *Phys. Rev. B*, Ithaca, N. Y., **8**(2):553-61, 1973.
8. KITTEL, C. *Introduction to solid state physics*. 4ed. New York, Wiley, 1971.
9. LEHMANN, C. Zur Bildung von Defekt-Kaskaden in Kristallen beim Beschuss mit energiereichen Teilchen. *Nukleonik*, Berlin, **3**:1-14, 1961.
10. LOMER, J. N. & PEPPER, M. Anisotropy of defect production in electron irradiated iron. *Phil. Mag.*, London, **16**:1119-28, 1967.
11. LUCASSON, P. G. & WALKER, R. M. Production and recovery of electron induced radiation damage in a number of metals. *Phys. Rev.*, Ithaca, N. Y., **127**(2):485-500, 1962.

12. _____ & WALKER, R. M. Variation of radiation damage parameters in metals *Phys. Rev.*, Ithaca, N. Y., 127(4):1130-6, 1962.
13. MEISSNER, D. *Defektproduktion und Erholung bei Tieftemperatur-Elektronenbestrahlung von Tantal*. Jülich, Kernforschungsanlage, Feb. 1970. (JüL-642-FN). [Thesis].
14. MILLER, M. G. & CHAPLIN, R. L. Defect production in vanadium by low energy electron irradiations *Radiat. Effects*, London, 22:107-8, 1974.
15. NEELY, H. H. & BAUER, W. Electron-irradiation damage-rate measurement in aluminum. *Phys. Rev.* Ithaca, N. Y., 149(2):535-9, 1966.
16. REED, R. E. et alii. Interlaboratory program to study low-temperature damage rates in dilute vanadium, niobium, and molybdenum alloys. In: SOLID State Division, annual progress report for period ending December 31, 1973. Oak Ridge, Oak Ridge National Lab., May 1974. (ORNL 4952).
17. RIZK, R. et alii. Displacement mechanisms in electron irradiated molybdenum *Physica St. Solidi A*, New York, 18:241-6, 1973.
18. WURM, J. *Bestimmungen der Verlagerungsfunktion in Aluminium und Kupfer aus Messungen der Defekterzeugung bei Tieftemperatur-Elektronenbestrahlung*. Jülich, Kernforschungsanlage, März 1961. (JüL-581-FN).
19. YOUNGBLOOD, G. et alii. Measurements of the threshold displacement energy in Ta and Nb. *Phys. Rev.*, Ithaca, N. Y., 188(3):1101-7, 1969.

